Available online at www.sciencedirect.com
SCIENCE DIRECT®
Acta Materialia 53 (2005) 1535–1544
Acta MATERIALIA
www.actamat-journals.com

Triple junction motion and grain microstructure evolution

G. Gottstein [a,*], Y. Ma [a], L.S. Shvindlerman [a,b]

[a] Institut für Metallkunde und Metallphysik, RWTH Aachen, Kopernikusstr. 14, D-52056 Aachen, Germany
[b] Institute of Solid State Physics, Russian Academy of Sciences, Chernogolovka, Moscow Distr. 142432, Russia

Received 26 November 2004; accepted 3 December 2004
Available online 5 January 2005

Abstract

The classical concepts of grain growth in polycrystals are based on the dominant role of grain boundaries. This is reflected by the well known von Neumann–Mullins relation. According to this approach triple junctions do not affect grain boundary motion, and their role in grain growth is reduced to maintaining the thermodynamically prescribed equilibrium angles at the lines where boundaries meet. In the current study the experimental data of triple junction mobility are considered with respect to the process of grain growth in 2D systems, in particular with regard to the controlling kinetics. When boundary kinetics prevails grain growth in a polycrystal complies with the von Neumann–Mullins relation. When grain growth is governed by the mobility of triple junctions the kinetics change, and the von Neumann–Mullins relation does not hold anymore. This is the more pronounced the smaller the triple junction mobility. We present a generalized theory of 2D grain growth including a limited triple junction mobility. In this concept the criterion Λ plays a central role. It reflects the ratio of boundary to triple junction mobility but is proportional to the grain size as well. The generalized von Neumann–Mullins relation can be expressed in terms of Λ. For small values of Λ, conspicuous changes of microstructure evolution during grain growth and of microstructural stability are predicted. The theoretical predictions are compared to results of computer simulations by a virtual vertex model.

Keywords: Grain boundary; Triple junction; Mobility; Grain growth

1. Introduction

Since metals are not transparent, we are used to imaging crystalline microstructures by means of 2D sections, for instance in optical micrographs. Although a number of approaches have been developed for quantitative analysis of a real 3D microstructure from 2D sections [1], the 2D image provides the basis for our understanding of the thermodynamics and kinetics of grain structure evolution. However, 2D grain microstructures are not a pure mathematical abstraction. In modern materials science objects with 2D grain structure are physically meaningful and have achieved great importance. Transformer sheet, thin films, coatings and thin layers are prominent examples of objects with 2D grain microstructures.

For a variety of problems it is possible to obtain an exact physical solution for 2D microstructures [2,3]. One conspicuous example is the classical von Neumann–Mullins relation of 2D grain growth kinetics [4,5], which determines the rate $\dot{S}$ of change of the grain area,

$$\dot{S} = -A_b\left(2\pi - \frac{n\pi}{3}\right) = \frac{A_b\pi}{3}(n-6), \tag{1}$$

where $A_b \equiv m_b\gamma_b$ is the reduced grain boundary mobility, m_b is the grain boundary mobility, γ_b is the grain boundary surface tension, n is the number of triple junctions of the considered grain, i.e., the topological class of the

* Corresponding author. Tel.: +492418026860; fax: +492418022608.
E-mail address: gottstein@imm.rwth-aachen.de (G. Gottstein).
URL: http://www.imm.rwth-aachen.de.

1359-6454/$30.00
doi:10.1016/j.actamat.2004.12.006

grain. Accordingly, the rate of area change is independent of the shape of the boundaries and determined by the topological class n only. Grains with $n > 6$ will grow, and those with $n < 6$ will disappear [4,5].

This relation describes the kinetics of grain microstructure evolution and constitutes a basis for practically all theoretical and experimental investigations as well as computer simulations of microstructural evolution in 2D polycrystals in the course of grain growth [6–8]. The relation (1) is based on three fundamental assumptions, namely:

(1) all grain boundaries possess equal mobilities (m_b) and surface tensions (γ_b), irrespective of their misorientation and the crystallographic orientation of the boundaries;
(2) the mobility of a grain boundary is independent of its velocity;
(3) the triple junctions do not affect grain boundary motion; therefore, the contact angles at triple junctions are always in equilibrium and, due to the first assumption, are equal to 120°.

The first assumption agrees with the so-called uniform boundary model and is likely to be realized in many cases. Of course, grain boundary mobility is significantly affected by grain boundary character [9], and an anisotropy of grain boundary properties manifests itself also in grain microstructure evolution [10]. Nevertheless, in polycrystals with random texture and in commercial alloys non-special boundaries are likely to prevail [11–13]. For a more refined analysis, anisotropic boundary properties also have to be taken into account, which, however, will not change the fundamental conclusions of the approach presented in the following.

The second assumption complies with the principles of absolute reaction rates. The third assumption is a mere hypothesis and needs to be checked experimentally. For this it is necessary to measure the triple junction mobility. The theoretical approaches and experimental techniques which make it possible to study the steady-state motion of grain boundary systems with triple junction were put forward and developed in [14–18]. It was shown that the behaviour of a grain boundary system with triple junction is determined by the dimensionless criterion $\Lambda = m_{tj}a/m_b$, where m_{tj} is the triple junction mobility, and a is the grain size:

$$\Lambda = \frac{2\theta}{2\cos\theta - 1}, \quad n < 6, \tag{2}$$

$$\Lambda = -\frac{\ln\sin\theta}{1 - 2\cos\theta}, \quad n > 6. \tag{3}$$

The link between parameter Λ and the angle θ at the tip of a triple junction makes it possible to measure the value of Λ and, in turn, the triple junction mobility for different metals and grain boundary systems [14,17]. It was found that the triple junction mobility is finite and may be low. Triple junction migration experiments were complemented by molecular dynamics simulation studies of the migration of grain boundaries with triple junctions. The simulations confirmed that the triple junction mobility can be limited and sufficiently low to affect the rate of grain boundary migration [19–22]. It is emphasized that the molecular dynamics simulation studies of triple junction migration were performed for the same geometrical configurations as used in experiment. On the whole, the simulations support the experimental observations of non-equilibrium triple junction angles and ascertain a substantial triple junction drag [14–17].

2. The generalized von Neumann–Mullins relation

Since the third assumption made to derive the von Neumann–Mullins relation can obviously be violated, it is of interest to consider the von Neumann–Mullins relation for the case of non-equilibrium contact angles at the triple junction. To conserve the central idea of the von Neumann–Mullins relation, let us consider a situation when the influence of the triple junction is rather large, but nevertheless, the motion of the system can be viewed as grain boundary motion, since the driving force is still due to grain boundary curvature, i.e., the role of the triple junction is reduced to a change of the angle θ. Grain boundary migration affected by triple junction drag can be considered as motion of a boundary with mobile defects [18], i.e.,

$$\dot{S} = -\frac{A_b}{1 + \frac{1}{\Lambda}}[2\pi - n(\pi - 2\theta)]. \tag{4}$$

Obviously the expression for the rate of area change will be different for grains with $n < 6$ and $n > 6$. Since the limited triple junction mobility reduces the steady state value of the angle θ as compared to the equilibrium angle, the shrinking rate of grains with $n < 6$ decreases. For grains with $n > 6$ triple junction drag increases the angle θ and also reduces the growth rate of such grains. In other words, microstructural evolution is slowed down by triple junction drag for any n-sided grain. Since the actual magnitude of θ is determined by triple junction and grain boundary mobility as well as the grain size there is no unique border between vanishing and growing grains with respect to their topological class anymore.

Since $\Lambda = \Lambda(\theta)$ we can find the relation between the rate of grain area change and the value of Λ, combining Eq. (4) with Eqs. (2) and (3), respectively. Close to equilibrium ($\theta = \pi/3$) we can obtain an explicit expression for $\theta(\Lambda)$ by expanding the function $2\cos\theta - 1$ into a power series in the vicinity of $\theta = \pi/3$ for $n < 6$ and $n > 6$, respectively, and neglecting higher order terms. For $n < 6$,

$$2\theta = \Lambda(2\cos\theta - 1)$$
$$\cong \Lambda\left[(2\cos\theta - 1)_{\theta=\pi/3} + (-2\sin\theta)_{\theta=\pi/3}(\theta - \pi/3) + \cdots\right] \tag{5}$$

or

$$\theta = \frac{\sqrt{3\pi}\Lambda}{6 + 3\sqrt{3}\Lambda} \tag{6}$$

and, therefore, with Eq. (4),

$$\dot{S} = \frac{m_b\gamma_b\pi}{3\left(1 + \frac{1}{\Lambda}\right)}\left(n\frac{6 + \sqrt{3}\Lambda}{2 + \sqrt{3}\Lambda} - 6\right). \tag{7}$$

For $\Lambda \to \infty$ – free boundary kinetics regime – Eq. (7) is identical with the classical von Neumann–Mullins relation.

We obtain for the topological class n^* of grains for which $\dot{S} = 0$,

$$n^* = \frac{2 + \sqrt{3}\Lambda}{1 + \frac{\sqrt{3}}{6}\Lambda}. \tag{8}$$

Evidently, n^* decreases with Λ, and for $\Lambda \to \infty$ $n^* \to 6$. For $n > 6$ Eq. (3) yields

$$\frac{1}{\Lambda} = \frac{2\cos\theta - 1}{\ln\sin\theta} \cong \left(\frac{2\cos\theta - 1}{\ln\sin\theta}\right)_{\theta=\pi/3} + \left[\frac{(-2\sin\theta)\ln\sin\theta - (2\cos\theta - 1)\cot\theta}{(\ln\sin\theta)^2}\right]_{\theta=\pi/3}(\theta - \pi/3) + \cdots \tag{9}$$

and in 1st order approximation,

$$\frac{1}{\Lambda} = \left(-\frac{2\sin\theta}{\ln\sin\theta}\right)_{\theta=\pi/3}(\theta - \pi/3) = -\frac{\sqrt{3}}{\ln\sin\pi/3}(\theta - \pi/3) \tag{10}$$

or

$$\theta = \pi/3 + \frac{1}{\Lambda B}, \tag{11}$$

where $B = -\frac{\sqrt{3}}{\ln\sin\pi/3}$ and with Eq. (4),

$$\dot{S} = \frac{m_b\gamma_b\pi}{3\left(1 + \frac{1}{\Lambda}\right)}\left[n\left(1 - \frac{6}{\pi\Lambda B}\right) - 6\right]. \tag{12}$$

As for $n < 6$, also for $n > 6$ Eq. (12) also becomes identical with the von Neumann–Mullins relation for $\Lambda \to \infty$ and the value of n^* reads

$$n^* = \frac{6}{1 - \frac{6}{\pi\Lambda B}}. \tag{13}$$

In this case n^* grows with decreasing Λ but $n \to 6$ for $\Lambda \to \infty$.

It is seen that the drag effect of grain boundary triple junctions results in a change of the topological limit between the classes of shrinking and growing grains such that the limit decreases for shrinking grains but increases for growing grains. This behavior $n^*(\Lambda)$ becomes obvious from Fig. 1, where the cases $n < 6$ and $n > 6$ are distinguished as $n_L^*(\Lambda)$ and $n_H^*(\Lambda)$, respectively.

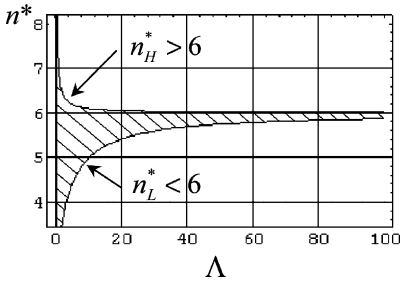

Fig. 1. Dependence of n_H^* and n_L^* on Λ.

3. Grain stability

Since there is a gap between n_L^* and n_H^* it is an interesting question as to how grains behave with $n_L^* < n < n_H^*$. From the above discussion it appears that such grains are neither capable to grow nor to shrink (Fig. 1), i.e., grains of the topological classes in the hatched area of Fig. 1 will be stable. This can be understood from the following consideration.

According to Eq. (4) $\dot{S}$ becomes zero for

$$\theta = \frac{\pi}{2}\left(1 - \frac{2}{n}\right). \tag{14}$$

For any integer n, $\theta(n)$ is exactly the (half) junction angle for an n-sided polygon, i.e., $\theta = 60°$ (=π/3) for $n = 6$, $\theta = 54°$ (=3π/10) for $n = 5$, $\theta = 45°$ (=π/4) for $n = 4$, $\theta = 67.5°$ (=3π/8) for $n = 8$, etc.

This means for a given (integer) n^* the angle θ corresponds to the (half) internal angle of an n^*-sided polygon, i.e., the boundaries are flat, and without curvature the polygon is stable.

The important point to consider is that the angle θ is a dynamic angle, i.e., it develops during motion of the boundaries that are connected at the triple junction. Prior to motion boundaries at a triple junction will adjust θ to attain the equilibrium angle ($\theta = 60°$). Therefore, 6-sided grains have flat boundaries, $n < 6$-sided grains have convex boundaries, $n > 6$-sided grains have concave boundaries. If the system is allowed to move the curved boundaries will move and adjust θ to the dynamic value, which is less than 60° for $n < 6$ and larger than 60° for $n > 6$.

The 6-sided grain will not change since it has flat boundaries to begin with, so there is no driving force for grain boundary motion and, therefore, no change of $\theta = \pi/3$. Let us consider a 5-sided grain under the condition $n^* = 4$, i.e., a 4-sided grain will attain flat

boundaries and, therefore, is stable (Fig. 2). Prior to motion the 5-sided grain has convex boundaries with $\pi/3 = \theta$ at the junctions. Triple junction drag will change the angle to $\theta = \pi/4$. Corresponding to $n^* = 4$, the angle $\theta = \pi/4 = 45°$ is smaller than the junction angle for a 5-sided grain with flat boundaries. During the change of the angle from initially $\theta = 60°$ to $\theta = 45°$ for the given Λ, the angle will pass through $\theta = 54°$, where the boundaries become flat and the driving force ceases. The configuration is locked. The junction angle may return to $\theta = 60°$ to establish static equilibrium at the junction, but this will make the boundary convex and drive the junction angle back to 54°. In essence, if the 5-sided grain were to attain the angle $\theta = 45°$ from initially 60°, it would have to change the curvature from convex to concave. For this to happen it must pass through a flat configuration, where the driving force ceases and the system becomes locked.

The same holds for a grain with $n^* > 6$. Let us consider $n^* = 8$ and a 7-sided grain. Initially, θ is in static equilibrium with $\theta = 60°$. The boundaries are concave. Because of $n^* = 8$ the dihedral angle of the 7-sided grain will change to a terminal 67.5°. At $\theta = 5\pi/14 = 64.3°$ the 7-sided grain will arrive at a configuration with flat boundaries. Again, the boundaries at static equilibrium are concave. A 7-sided grain for $\theta = 67.5°$ with a Λ corresponding to $n^* = 8$ would have convex boundaries. It never can get there, since the change in curvature requires a transient flat boundary, where the system will become locked, when only curvature drives the boundary system.

In summary, grains with n sides with $n_L^* < n < n_H^*$ become locked and can neither grow nor shrink. This phenomenon might be essential for understanding the high stability of grain microstructure in ultrafine grained and nanocrystalline materials, specifically in 2D thin layers and films. For $\Lambda \to \infty$, i.e., for $\theta = \pi/3 = \text{const.}$, the border between growing and shrinking grains is the singular value $n^* = 6$. It dissociates to an interval (between n_L^* and n_H^*) for $\Lambda \ll \infty$. Such an effect is expected to further stabilize the grain microstructure. Since Λ depends on grain size, this stabilization is more pronounced in fine grained and nanocrystalline systems.

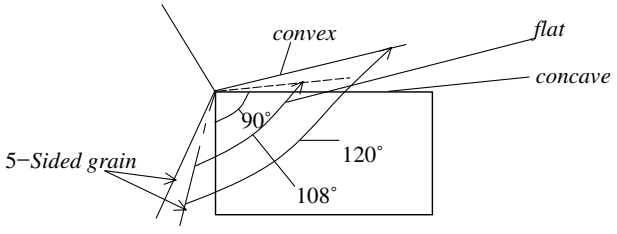

Fig. 2. Geometry of a 5-sided grain during transition from static to dynamic equilibrium for $n^* = 4$.

4. Triple junction controlled growth

So far we have considered the motion of a grain boundary system with triple junctions in the case where the system moves under boundary kinetics while triple junctions only slightly disturb the motion of the system. In the following we shall consider the case when the motion of grain boundaries is controlled by the motion of triple junctions. To begin with we will show that under triple junction control in the course of grain growth in 2D systems the grains will eventually be bordered by straight (flat) boundaries, i.e., they will assume a polygonal shape.

Let us consider the curvature κ of a grain boundary system with triple junctions (for the configurations which relate to $n < 6$ and $n > 6$). As derived in [18] for the system with $n < 6$ we obtain with $\xi = a/2\theta$,

$$\kappa = \frac{1}{\xi} e^{-x/\xi + \ln \sin\theta} = \frac{2\theta}{a} e^{-(2\theta/a)x} \sin\theta = \frac{\Lambda}{a} \sin\theta (2\cos\theta - 1) e^{-(2\theta/a)x}, \quad (15a)$$

while for the system with $n > 6$ it was shown that,

$$\kappa = \frac{\ln \sin\theta}{x_0} e^{(x/x_0)\ln\sin\theta} = \frac{\Lambda}{x_0}(1 - 2\cos\theta) e^{(x/x_0)\ln\sin\theta}. \quad (15b)$$

Since for triple junction kinetics $\Lambda \to 0$, also the grain boundary curvature κ approaches zero, i.e., the grain structure of 2D polycrystals comprises straight grain boundaries. In other words, under triple junction kinetics the grains in a 2D polycrystal represent a system of contiguous polygons.

More specifically, as shown in [18], in the framework of triple junction kinetics a polygon of arbitrary shape will be transformed into an equilateral polygon, and any deviation from an equilateral polygon will generate a force to restore the equilibrium shape. The only exception is a triangle, i.e., a grain of topological class $n = 3$ is always unstable and must disappear. Eventually, all other shrinking polygons must by necessity go through this stage, when grain growth is controlled by the motion of triple junctions.

This phenomenon has important consequences for the development of grain growth. To demonstrate this we take a look at the evolution of a shrinking grain in the course of grain growth. The topological class of such a grain must be lower than 6, naturally taking into account all corrections to the von Neumann–Mullins relation, given above. We emphasize that the transition between boundary and triple junction kinetics does not only depend on grain boundary and triple junction mobility, but on the size of a grain as well. When the size of a grain diminishes progressively there comes a time when boundary kinetics becomes replaced by junction kinetics. This will happen to grains of the topological

class $n = 4$ or $n = 5$ which are bound to shrink even after such a transition to triple junction kinetics. Grains of topological class $n = 3$ will collapse without transforming into a regular polygon. Since the kinetics of triple junctions is significantly slower than boundary kinetics, the 4- and 5-side polygons will shrink, and eventually contract to a point although at a markedly smaller rate. How this phenomenon reveals itself during grain growth will be considered below.

Let us finally consider the behavior of a regular n-sided polygon with an interior and exterior circle of radius $\tilde{r}$, respectively $\tilde{R}$. As shown in [18], the rate of grain area change $\dot{S}$ can be expressed as

$$\dot{S} = -m_{\mathrm{tj}}\gamma n\tilde{R}\sin\left(\frac{2\pi}{n}\right)\left[2\sin\left(\frac{\pi}{n}\right)-1\right] = -2m_{\mathrm{tj}}\gamma n\tilde{r}\sin\left(\frac{\pi}{n}\right)\left[2\sin\left(\frac{\pi}{n}\right)-1\right]. \quad (16)$$

In essence, a limited triple junction mobility always slows down the evolution of grain microstructure of polycrystals, irrespective of whether the topological class of the considered grain is smaller or larger than 6. Formally, for grains with $n < 6$, the sluggish motion of the triple junctions "reduces" the effective topological class of growing grains, while for grains with $n > 6$ the triple junction behavior makes the topological class of vanishing grains appear larger.

The mere fact that there is a growing grain with triple junctions of low mobility requires the existence of other grains with $n < 6$ to surround it. There is no point in discussing to which grain their common junction belongs. The only exception holds for $n = 6$, since under triple junction control a hexagonal grain structure with contact angle $2\theta = 2\pi/3$ becomes unstable. Since the actual magnitude of Λ is determined by the triple junction and grain boundary mobility as well as by the grain size and is independent of the number of sides of a grain, there is no unique dividing line between vanishing and growing grains with respect to their topological class anymore, like $n = 6$ in the von Neumann–Mullins approach. As has been detailed above for sufficiently small Λ the border between shrinking and growing grains degenerates to an interval bounded by the lines $n^*_{\mathrm{H}}(\Lambda)$ and $n^*_{\mathrm{L}}(\Lambda)$ (Fig. 1) which contracts to a point for $\Lambda \to \infty$.

5. Applications

5.1. Theoretical predictions

In the following we consider the consequences of the two approaches for the evolution of granular microstructures. The distinguishing feature of the von Neumann–Mullins model is the infinite mobility of grain boundary triple junctions. This requires that grains in a "von Neumann–Mullins polycrystal" are bordered by curved boundaries. This should manifest itself in linear dependences of the mean grain area on time and of the rate of grain area change on the topological class. For a given reduced boundary mobility $A_{\mathrm{b}} = m_{\mathrm{b}}\gamma_{\mathrm{b}}$ a grain with topological number n is characterized by a unique value of its rate of area change $\mathrm{d}S/\mathrm{d}t = \dot{S}$. The slope of the relation $\dot{S}(n)$ is only determined by the reduced grain boundary mobility: $\mathrm{d}\dot{S}/\mathrm{d}n = m_{\mathrm{b}}\gamma_{\mathrm{b}}\pi/3$. (We would like to remind the reader that both the von Neumann–Mullins model and our model are based on the uniform grain boundary and triple junction approach.)

In the opposite case, for pure triple junction kinetics the grains in a 2D polycrystal are bordered by straight lines, i.e., the grain microstructure is represented by a system of space filling polygons. The temporal evolution of such a system is defined by Eq. (16).

A practically relevant and theoretically most interesting case is an intermediate situation, when the triple junction influence is tangibly large, but nevertheless, the evolution of the system can be still considered as governed by grain boundary motion. In this case the time dependence of the average grain area $\langle S\rangle$ is practically linear, however, the rate of grain area change $\dot{S}$ is defined not only by the topological class n but by the criterion Λ as well (Eq. (4) with (2) and (3) respectively, (7), (12)). So, there is no unique relation anymore between $\dot{S}$ and topological class n of the grain; the dependence $\dot{S}(n)$ is blurred by the impact of criterion Λ.

The discussed consequence afforded by the developed approach is probably the most significant one, but the new approach also allows us to make some more quantitative predictions:

- Grains are neither capable to grow nor to shrink in the intermediate situation that manifests itself in the dependency $n^*(\Lambda)$.
- Under triple junction kinetics grains should be bordered by flat boundaries, i.e., straight lines in 2D.
- Under triple junction kinetics a system of polygons tends to transform to a system of equilateral polygons. The only exception is the triangle which will collapse without transforming into a regular polygon.
- For triple junction kinetics the rate of grain area change can be described by Eq. (16).

5.2. Computer simulations

In both theoretical approaches only a single grain and its behavior is considered in an unspecified, i.e., average environment. To study the effect of discrete granular arrangements we employed computer simulations of 2D grain growth. Curvature and boundary tension driven grain growth is best represented by a (virtual) vertex model [23–25]. In such a model the driving force is the net grain boundary surface tension at a

vertex. A vertex can be a triple junction or any point on a polygonized grain boundary. For a given time interval the equation of motion is solved concomitantly for all vertices. Each vertex is assigned a mobility so that different mobilities for triple junctions and boundaries can easily be implemented.

In Fig. 3 the simulated evolution of the microstructure of a 2D polycrystal is presented at various stages of grain growth. The evolution was fully controlled by grain boundary kinetics. The time dependence of the mean grain area was computed. As is apparent from Fig. 3(a), the grains are bordered by curved boundaries. The dependence of the mean grain area on time, and especially the dependence of the rate of grain area change $\dot{S}$ vs. the topological class n of a grain are shown in Fig. 3(b) and (c). They reflect all features that are peculiar to a "von Neumann–Mullins polycrystal": $\langle S\rangle$ increases linearly with annealing time; the rate of grain area change $\dot{S}$ is linear in n, and the line $\dot{S}(n)$ intersects the axis n at $n = 6$, i.e., $\dot{S} = 0$ at $n = 6$. The slope of the line $\dot{S}(n) = \pi m_b \gamma_b/3$ is as predicted by the von Neumann–Mullins relation. In essence, for boundary controlled grain growth of a homogeneous system the von Neumann–Mullins approach is convincingly reproduced.

In order to study the effect of triple junction mobility on grain growth, two situations were considered. The first case related to the kinetics, when the triple junction influence is tangibly large, but nevertheless, the evolution of the system can be described as a result of curvature driven grain boundary motion. In contrast to unconstrained grain boundary motion, however, the boundaries are much more straight (Fig. 4(a)). When Λ is still relatively large, $0.4 \leqslant \Lambda \leqslant 5.0$, the mean grain area $\langle S\rangle$ changes linearly with time t, which reflects the nature of the controlling grain boundary kinetics of the system at this stage (Fig. 4(b)). The quantitative variation of the rate of grain area change $\dot{S}$ on topological class n, which is a straight line for pure grain boundary kinetics (Fig. 3(c)) is transformed to an area under the constraint of a finite triple junction mobility (Fig. 4(c)). For all topological classes a large scatter of $\dot{S}(n)$ is observed. While for unconstrained grain boundary kinetics (infinite junction mobility) $\dot{S}$ is a function of n only, for a system with finite junction mobility $\dot{S}$ becomes a function of both n and Λ, $\dot{S} = \dot{S}(n, \Lambda)$ (Fig. 4(c)). The straight line in Fig. 4(c), which describes the von Neumann–Mullins relationship, has the slope $\pi m_b \gamma_b/3$ and $\dot{S}(n = 6) = 0$.

As the parameter Λ decreases the influence of triple junction drag becomes obvious not only in the $\dot{S}$–n diagram, but also in changes of the dependency $\langle S\rangle(t)$ (Fig. 5). Hence, grain growth cannot be considered anymore to be controlled by boundary kinetics affected by triple junction drag, rather the dependency $\dot{S}_n(\Lambda)$ clearly demonstrates that a finite triple junction mobility fundamentally changes the character of the function. For a given n, $\dot{S}(\Lambda)$ is not represented by a point anymore, but by a line (Fig. 6). There are two

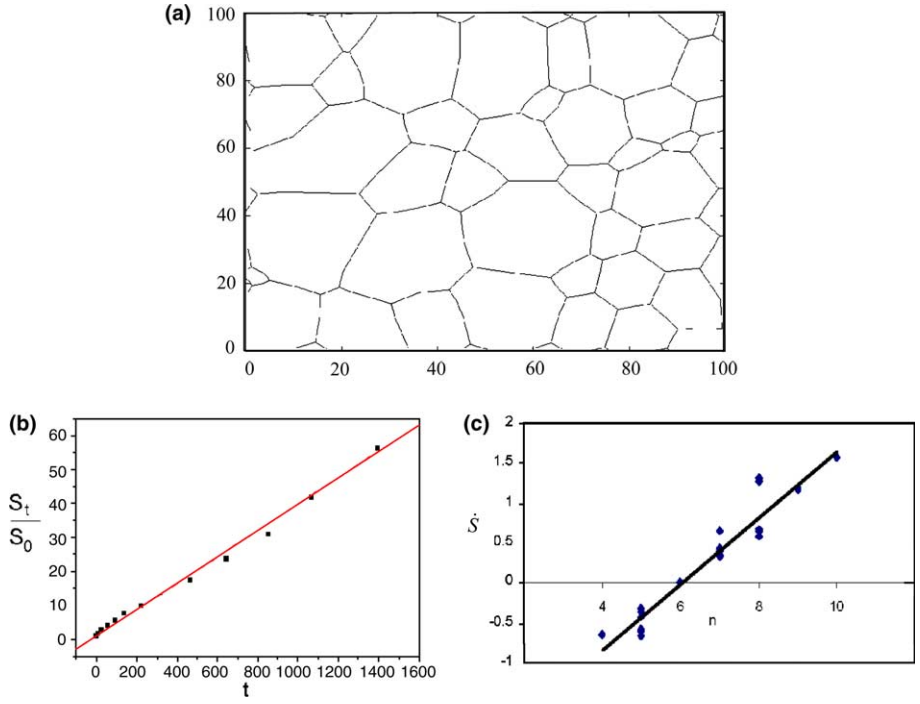

Fig. 3. Simulation results for a 2D polycrystal for grain boundary kinetics ($\Lambda \to \infty$): (a) Microstructure at $S_t/S_0 = 17.2$; (b) normalized area S_t/S_0 vs. time t; (c) $\dot{S}$ as function of n.

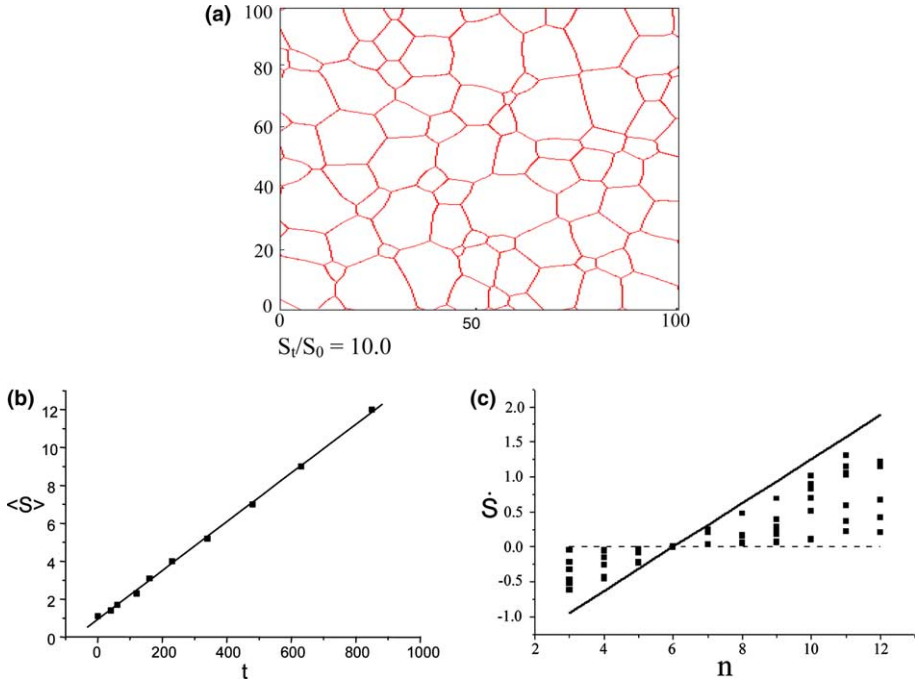

Fig. 4. Simulation result for $0.1 < \Lambda < 1.0$: (a) Microstructure at $S_t/S_0 = 10.0$; (b) average area $\langle S \rangle$ vs. time t; (c) $\dot{S}$ as function of n for $0.1 < \Lambda < 10$. Solid squares are the results of computer experiments, the line represents the von Neumann–Mullins relation.

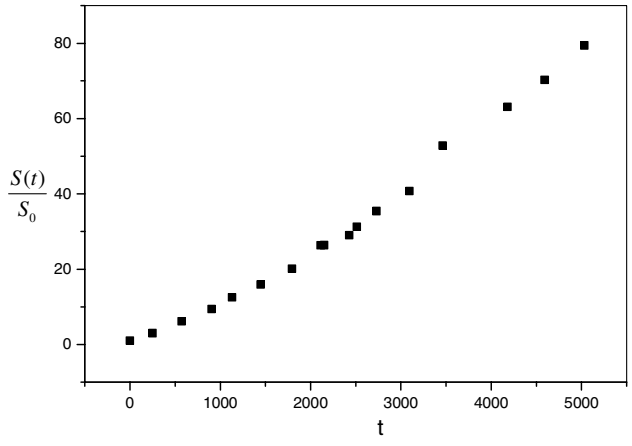

Fig. 5. Grain size vs. time for $0.01 < \Lambda < 1.0$.

issues which should be stressed. Firstly, a good agreement between the computer experiment and theory is observed. Further, according to the presented theoretical approach Eqs. (2) and (4) (or (7) and (12)) perfectly describe in close proximity to equilibrium, i.e., for rather large Λ, the influence of a finite triple junction mobility on the rate of grain area change, $\dot{S}_n$, given that all von Neumann–Mullins conditions, except the infinite triple junction mobility, are fulfilled. The expressions:

$$\lambda_{n<6} \equiv \frac{\dot{S}^{\mathrm{TJ}}_{n<6}}{\dot{S}^{\mathrm{VNM}}_{n<6}} \simeq \frac{n\frac{6+\Lambda\sqrt{3}}{2+\Lambda\sqrt{3}}}{n-6}, \tag{17a}$$

$$\lambda_{n>6} \equiv \frac{\dot{S}^{\mathrm{TJ}}_{n>6}}{\dot{S}^{\mathrm{VNM}}_{n>6}} \simeq \frac{n\left(1-\frac{6}{\pi AB}\right)-6}{n-6}, \tag{17b}$$

represent the ratio of the rate of grain area change for finite triple junction mobility and for the pure von Neumann–Mullins case. For the same value of Λ, grains with $n < 6$ deviate more strongly from pure grain boundary kinetics than do grains with $n > 6$. Therefore, grains with $n = 4$ are under triple junction control (Fig. 6), while the growth of grains with $n = 9$ is governed by boundary kinetics (Fig. 6). In other words, triple junction drag not only slows down the rate of grain growth, but changes the grain microstructure of 2D polycrystals. This is also evident in experimental observations of grain growth in thin foils [26]. At the stage of the process where triple junction influence becomes obvious, i.e., when the time dependency of the mean grain size is linear, the grain size distribution becomes wider.

For grain growth strictly controlled by triple junction motion, theory predicts that the grain boundaries become flat and that the grains approach a shape of equilateral polygons. A polygon of arbitrary shape will be transformed into an equilateral polygon, and any deviation from an equilateral polygon will generate a force to restore the equilibrium shape. The only exception is a triangle, i.e., a grain of topological class $n = 3$ is always unstable and bound to disappear. The computer simulations fully confirm the theoretical predictions. Fig. 7 represents the grain microstructure developed under triple

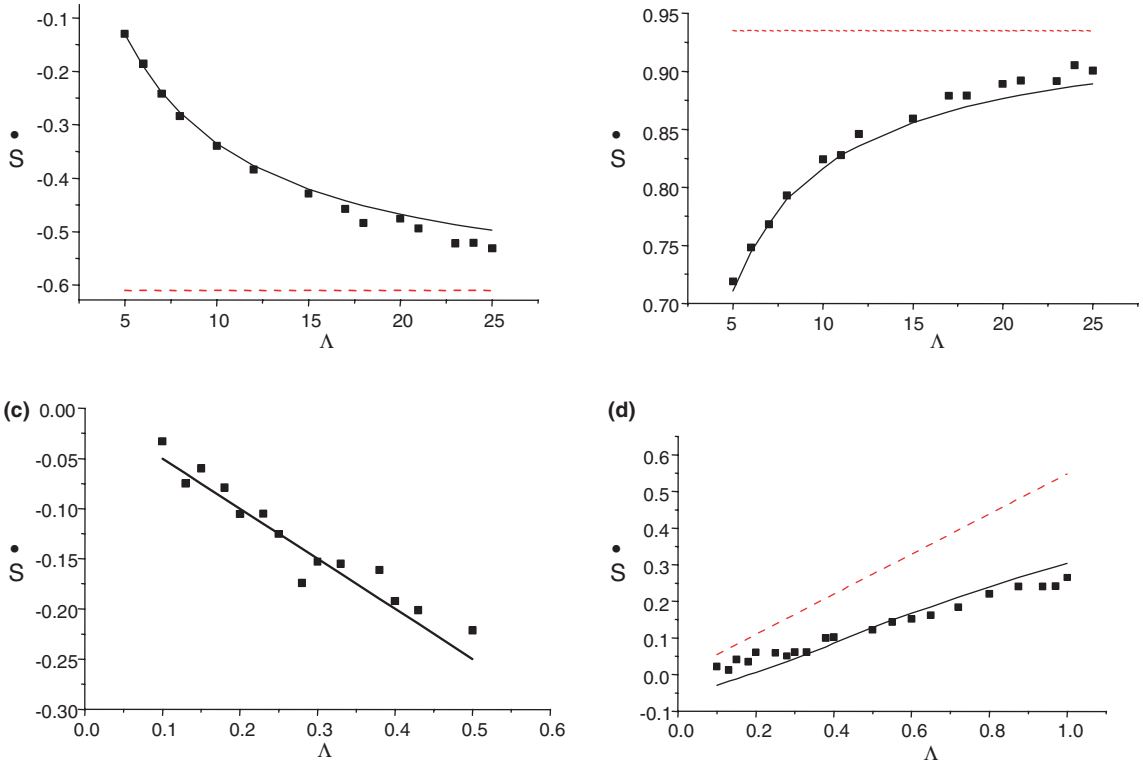

Fig. 6. The rate of grain area change $\dot{S}$ as a function of Λ: (a) For grains with $n = 4$. Filled squares are the results of computer simulations. The solid line represents the theoretical prediction for intermediate kinetics (Eqs. (2) and (4)) ($5 < \Lambda < 25$), the dotted line corresponds to the von Neumann–Mullins relation. (b) For grains with $n = 9$. The solid line represents the theoretical prediction for intermediate kinetics (Eqs. (3) and (4)). The dotted line corresponds to the von Neumann–Mullins relation. (c) For grains with $n = 4$, and $0.1 < \Lambda < 1.0$. The solid line represents the theoretical prediction for triple junction kinetics (Eq. (16)). (d) For grains with $n = 9$. The solid line is the theoretical prediction for intermediate kinetics (Eqs. (3) and (4)), the broken line represents triple junction kinetics.

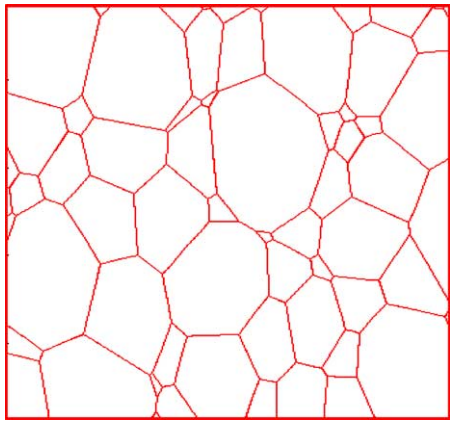

Fig. 7. Simulation results for a 2D polycrystal at $\Lambda \sim 10^{-4}$. Microstructure at $S_t/S_0 = 10.0$.

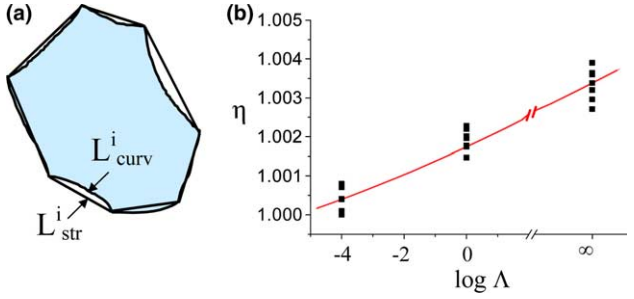

Fig. 8. Measure of boundary straightness: (a) diagram explaining how the value η was measured; (b) computer simulation (filled squares) up to $S_t/S_0 = 10$ and theoretical prediction (solid line) of $\eta(\log \Lambda)$.

junction kinetics. The grains are bordered by straight lines. The ratio,

$$\eta = \frac{\sum_{i=1}^{n} \frac{L^i_{\text{curv}}}{L^i_{\text{str}}}}{n},$$

gives a quantitative measure of grain boundary curvature, where L_{curv} is the length of a curved boundary and L_{str} is the distance between the two corresponding triple junctions (Fig. 8). When Λ tends to zero, $\eta \to 1$ (Fig. 8(b)).

To assess the theoretical prediction that under triple junction kinetics all 2D grains of arbitrary shape become converted to equilateral polygons – except for triangles – we define the parameter,

$$\beta_n = \frac{\frac{L_1}{L_2} + \frac{L_2}{L_3} + \cdots + \frac{L_{n-1}}{L_n} + \frac{L_n}{L_1}}{n}, \tag{18}$$

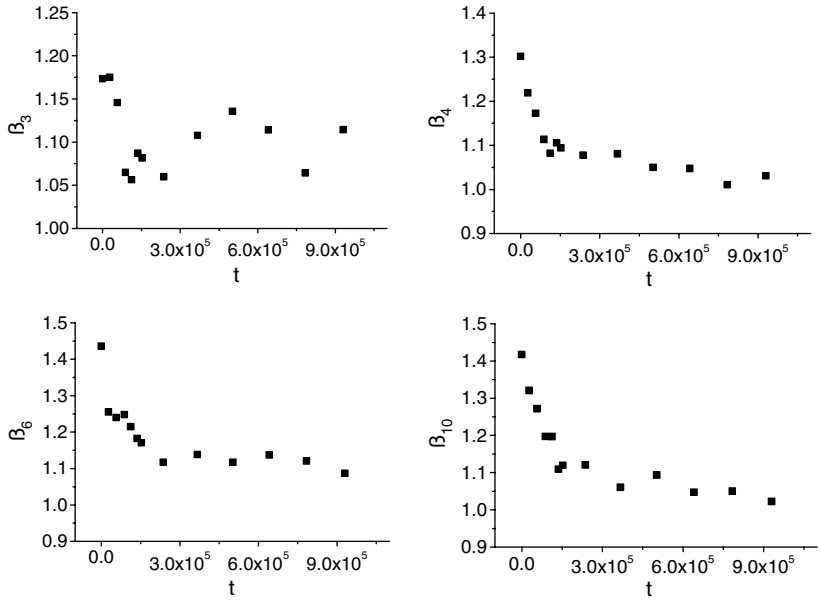

Fig. 9. Time dependence of β_n for various n under triple junction kinetics ($\Lambda \approx 10^{-4}$) up to $S_t/S_0 = 10$.

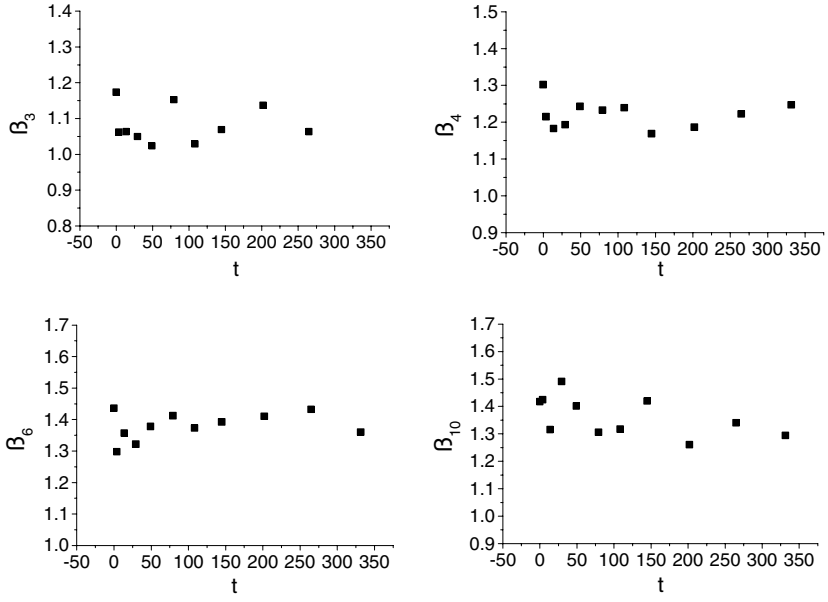

Fig. 10. Time dependence of the "rectilinearity" β_n under grain boundary kinetics ($\Lambda \gg 1$) for $S_t/S_0 = 10.0$.

where L_i is the length of the ith side of an n-sided grain. When the shape of a grain approaches an equilateral polygon, $\beta \to 1$. The only exception is a triangle, which is unstable and has to disappear, i.e., β_3 should not converge toward $\beta_3 = 1$. The behavior of β_n with time was determined from the computed microstructure, including β_3 (Fig. 9). Apparently for all studied n-sided polygons $\beta \to 1$, except for β_3 which changes randomly. Fig. 10 confirms that such behavior of β_n holds for triple junction kinetics only. The value β_n was measured up to $S_t/S_0 = 10$. As is apparent from Figs. 9 and 10 a grain size 10 times larger than the initial grain size was reached in a much shorter time for boundary kinetics.

The function $\dot{S}(n)$ for triple junction kinetics is presented in Fig. 11. The curve is calculated according to Eq. (16) while the symbols represent simulation results. Except for the intrinsically unstable triangular grains ($n = 3$), the theoretical predictions are in good agreement with the computer experiment. We note that $\dot{S}$ rises with n and approaches a limit (Eq. (16)) contrary to the predictions of the von Neumann–Mullins relation.

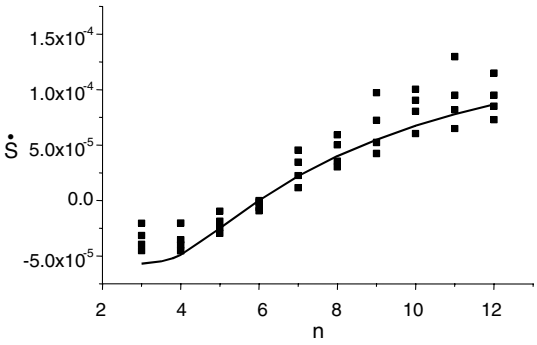

Fig. 11. $\dot{S}$ vs. topological class n. Simulation results (filled squares) for $\Lambda \sim 10^{-4}$. The solid line represents the dependency predicted by Eq. (16).

6. Summary

The motion of grain boundaries with triple junctions is considered. Particular emphasis is placed on the role of triple junction drag during grain growth and grain microstructure evolution. It is shown that the classical view of grain growth in polycrystals which is based on grain boundary motion only is inadequate to describe the process. A new theoretical concept is proposed that accounts also for limited triple junction mobility. Specifically, it was shown that a finite mobility of grain boundary triple junctions does not only slow down the grain growth rate but also changes microstructure evolution and topology. The predictions of the theoretical concept were found to compare well with computer simulations of 2D grain growth.

Acknowledgements

Financial assistance from the Deutsche Forschungsgemeinschaft (Grant Go335/10) is gratefully acknowledged. The cooperation was supported by the Deutsche Forschungsgemeinschaft (DFG Grant 436 RUS 113/714/0-1(R)) and the Russian Foundation of Fundamental Research (Grant DFG-RRFI 03 02 04000).

References

[1] Cahn RW, Haasen P, editors. Physical metallurgy. Amsterdam: North-Holland; 1996.
[2] Aristov VYu, Fradkov VE, Shvindlerman LS. Sov Phys Solid State 1980;22:1055.
[3] Verhasselt JCh, Gottstein G, Molodov DA, Shvindlerman LS. Acta Mater 1999;47:887.
[4] Mullins WW. J Appl Phys 1956;27:900.
[5] Von Neumann J. In: Metal interfaces. Cleveland: American Society for Testing Materials; 1952. p. 108.
[6] Lücke K, Heckelmann I, Abbruzzese G. Acta Metall Mater 1992;40:533.
[7] Anderson MP, Srolovitz DJ, Grest GS, Sahni P. Acta Metall 1984;32:783.
[8] Fradkov VE, Shvindlerman LS, Udler DG. Scripta Metall 1985;19:1285.
[9] Gottstein G, Shvindlerman LS. Grain boundary migration in metals: thermodynamics kinetics applications. CRC Press; 1999.
[10] Demirel MC, Kuprat AP, George DC, Rollet AD. Phys Rev Lett 2003;90(1):016106.
[11] Fridman EM, Kopetskii ChV, Shvindlerman LS. Zt Metallk 1975;66:533.
[12] Lejcek P, Adamek J. J Phys IV 1995;C3(5):107.
[13] Molodov DA, Czubayko U, Gottstein G, Shvindlerman LS. Acta Mater 1998;46:553.
[14] Czubayko U, Sursaeva VG, Gottstein G, Shvindlerman LS. Acta Mater 1998;46:5863.
[15] Gottstein G, Shvindlerman LS. Scripta Mater 1998;38:1541; Gottstein G, Shvindlerman LS. Scripta Mater 1998;39:1489.
[16] Gottstein G, King AH, Shvindlerman LS. Acta Mater 2000;48:397.
[17] Protasova SG, Gottstein G, Molodov DA, Sursaeva VG, Shvindlerman LS. Acta Mater 2001;49:2519.
[18] Gottstein G, Shvindlerman LS. Acta Mater 2002;50:703.
[19] Upmanyu M, Srolovitz DJ, Shvindlerman LS, Gottstein G. Interf Sci 1999;7:2307.
[20] Upmanyu M, Srolovitz DJ, Shvindlerman LS, Gottstein G. Acta Mater 2002;50:1405.
[21] Upmanyu M, Srolovitz DJ, Gottstein G, Shvindlerman LS. Interf Sci 1998;6:289.
[22] Upmanyu M, Srolovitz DJ, Shvindlerman LS, Gottstein G. Acta Mater 1999;47:3901.
[23] Kawasaki K, Nagai T, Nakashima K. Phil Mag 1989;60:399.
[24] Weygand D, Brechet Y. Phil Mag B 1998;78:329.
[25] Zheng M, Gottstein G. Aluminium 2002;78:878.
[26] Novikov VYu. Mater Sci Forum 2004;467–470:1093–8.